2640–2647 *Nucleic Acids Research, 1996, Vol. 24, No. 14*

DNA bending by the silencer protein NeP1 is modulated by TR and RXR

Rüdiger Arnold, Mark Burcin, Burkhard Kaiser, Marc Muller and Rainer Renkawitz*

Genetisches Institut der Justus-Liebig-Universität, Heinrich-Buff-Ring 58-62, D-35392 Giessen, Germany

Received May 6, 1996; Revised and Accepted May 29, 1996

ABSTRACT

NeP1 binds to the F1 silencer element of the chicken lysozyme gene and, in the presence of TR, v-ERBA or RAR, synergistically represses transcriptional activity. This repression involves a silencing mechanism acting independently of the relative promoter position. Here we show that NeP1 alone can induce a significant directed bend on DNA. The chicken homologue of human NeP1, CTCF, shows identical binding and bending properties. In contrast, the isolated DNA binding domain of CTCF efficiently binds DNA, but fails to confer bending. Similarly, the TR–RXR hetero- or homodimer, binding adjacent to NeP1 at the F2 sequence, do not show significant DNA bending. The binding of the T3 ligand to TR changes neither the magnitude nor the direction of the NeP1 induced bend. However, when all factors are bound simultaneously as a quaternary complex, the TR–RXR heterodimer changes the location of the bend center, the flexure angle and the bending direction.

INTRODUCTION

The –2.4 kb silencer of the chicken lysozyme gene is inactive in mature, lysozyme expressing macrophages, and is active in all other cell types tested. This activity correlates with the presence of a DNase I-hypersensitive site in the chromatin (1). The silencer DNA consists of two protein binding sites that are both required for full functional activity (2). One site is bound by NeP1, whereas the second site is bound by the thyroid hormone receptor (TR). These silencer modules are termed F1 and F2 respectively, and can repress gene activity independently from each other (2,3). The repression is increased synergistically when both modules are bound by their respective factors. NeP1 binds as a monomer to F1 (3) and TR binds as a homodimer or a heterodimer with the retinoid-x-receptor (RXR) to F2 (4,5). Synergistic repression is converted to synergistic induction in the presence of thyroid hormone (T3) (2).

Binding of NeP1 to DNA is characterized by an *in vitro* footprint region of ~50 bp interrupted by a DNase I-hypersensitive site (2,3). Therefore, we wondered whether such a long stretch of DNA might be bent by NeP1. Bending may be required for possible nucleosome binding and/or for the assembly of other interacting partners (6,7).

Here we analyzed bending effects of NeP1 binding to F1 in the absence or the presence of TR–TR homodimers or TR–RXR heterodimers. NeP1 shows a significant bending activity. In the presence of TR or TR–RXR the bending angle is reduced. In addition, as compared with the NeP1–DNA complex, the position and orientation of the bend is changed in the quaternary NeP1–TR–RXR complex.

MATERIALS AND METHODS

Protein sources

NeP1 was purified from HeLa cell nuclear extract and prepared as described (8,9). The nuclear proteins were applied onto a Q-Sepharose column to enrich NeP1. The fractions eluting from 350 to 500 mM NaCl were further fractionated with a heparin–Sepharose column. For both columns, HS-buffer (25 mM HEPES–KOH, pH 7.6, 5 mM $MgCl_2$, 1 mM EGTA, 1 mM DTT, 10% glycerol) was used. The resulting fractions with detectable NeP1 DNA binding activity in EMSA were eluted with 700 mM NaCl using a step gradient. After dialysis using binding buffer [10 mM HEPES, 10 mM KCl, 2.5 mM $MgCl_2$, 10% (w/v) glycerol, pH 7.6], the protein fractions were applied onto a F1 DNA-affinity column. Fractions eluting with 300 mM NaCl were used in all EMSA experiments as described below.

Human TRα1 was expressed in *Escherichia coli*. The pET-hTR-α1 vector (a kind gift from L. J. DeGroot) was transformed into the bacterial strain BL21(DE3)pLYS S (10). The culture was grown at 37°C to an O.D. of 0.4, IPTG was added to 0.5 mM final concentration and the culture was incubated for 5 h at 20°C with gentle agitation. Bacteria were harvested by centrifugation and the pellet was resuspended in 20 ml of lysis buffer (20 mM Tris, pH 8, 100 mM NaCl, 0.5 mM $MgCl_2$, 1 mM PMSF, 1% aprotinin). The suspension was sonicated on ice in order to obtain a clear lysate, 2 ml of DEN (0.1 M DTT, 0.5 M EDTA, 5% NP-40) was added and bacterial debris was removed by centrifugation at 60 000 *g*. Soluble proteins were precipitated from the supernatant by addition of 0.33 g/ml ammonium sulfate and recovered by centrifugation at 60 000 *g*. The pellet was resuspended in 1 ml HS buffer and the solution was dialyzed against HS buffer (see above). The fraction was loaded onto a heparin–Sepharose column and proteins were eluted using a linear KCl gradient. The fractions were tested for the presence of hTRα by a gel retardation assay using a DR-4 probe and by SDS–PAGE followed by Coomassie staining or western blotting. Eluates at 0.4–0.7 M KCl

* To whom correspondence should be addressed

contained a >95% pure preparation of bacterially expressed, soluble hTRα1.

Human RXRα was prepared by *in vitro* transcription and translation of pSG-hRXRα (11) using reticulocyte lysate in combination with the TNT-Kit (Promega). For the EMSA experiments, 2 µl of a translation reaction were used per lane.

Chicken full length CTCF and the CTCF DNA binding domain were expressed in COS-1 cells using the plasmids pSG5-CTCF, a kind gift from E. M. Klenova (12), and pABΔ-CTCF ZnFg (to be published elsewhere). COS 1-cells ($2–3 \times 10^6$) were transfected with 25 µg DNA using the standards protocols. After cultivation for 48 h the cells were collected, resuspended in 200 µl binding buffer (20 mM HEPES, pH 7.8, 400 mM KCl, 20% glycerol, 2 mM DDT) and frozen in cold methanol (–80°C). After thawing on ice and sedimenting the cell debris (11 000 r.p.m., 4°C, 10 min) the supernatant was used for EMSA (see below).

Probe construction

Oligonucleotides containing F1 and F2 modules were cloned into the *Hin*dIII/*Acc*I site of pBluescript II SK+ (Stratagene). The F2 oligonucleotide was orientated in sense relative to F1 and contains the natural 8 bp distance to the F1 module. The resulting pSK+ F1/F2s was partially digested with *Bss*HII and ligated with the purified *Bss*HII fragment of pSK+ F1/F2s to generate pSK+ $(F1/F2)_2$ with a dimerized polylinker region containing the F1/F2 modules. This plasmid was used for circular permutation analysis by digestion with the indicated restriction enzymes (see Fig. 2A). The resulting fragments of 281 bp were end-labelled with [α-^{32}P]dNTPs using Klenow enzyme. The radioactive fragments were cut out of a 5% polyacrylamide gel and eluted in TE buffer (10 mM Tris, 1 mM EDTA, pH 7.6) under gentle agitation for 15 h at room temperature.

Plasmids pRN169–174, used to generate phasing vectors, were provided from Rainer Niedenthal (13). Each plasmid contains three phased A-tracts, inducing an intrinsic bend, followed by a spacer region of 9, 11, 13, 15, 17 or 19 bp downstream of an *Eco*RV cleavage site. Intrinsic bend containing DNA fragments were generated by cutting pRN169–174 with *Eco*RV/*Bam*HI and ligating the DNA fragment into the *Eco*RV/*Bam*HI site of pSK+ F1/F2s. The resulting plasmids, pSK+P1–P6, were cleaved with *Bss*HII to generate the set of 296–306 bp long DNA fragments for the phasing analysis.

Electrophoretic mobility shift analysis

DNA–protein binding reactions for the electrophoretic mobility shift analysis (EMSA) were carried out in 40 µl 1× binding buffer (described above) supplemented with 1–4 µg salmon sperm DNA and 0.5–1.0 µg poly(dI–dC) depending on the incubated protein amounts. After preincubation for 15 min on ice, 15–40 fmol of each radioactive probe was added and incubated for 20 min at room temperature. DNA–protein complexes were analyzed on nondenaturating polyacrylamide gels [5% (w/v) acrylamide; 0.125% (w/v) bisacrylamide] in TBE buffer (90 mM Tris, 90 mM borate, 2 mM EDTA, pH 8.3). Electrophoresis was performed at 4°C with a field strength of 7 V/cm for 16 h.

Calculation of DNA flexure parameters

The mobilities of the complexes in the circular permutation and phasing analysis were corrected for any variation in probe mobilities by dividing the complex mobilities with the free probe mobilities. The resulting data were expressed relative to the complex with the highest mobility (14–17). In the case of circular permutation analysis, the data were plotted as a function of the distance from the middle of the F1 element to the nearest end of the fragment. The best fit to a cosine function was determined through PlotIt (Scientific Programming Enterprises, Haslett, MI, USA). Bend centers and standard errors were calculated using the resulting equations for the cosine functions. The DNA flexure angle (f) was determined by the equation $y_{min}/y_{max} = \cos(f/2)$ where y refers to the minimal (min) or maximal (max) relative mobility (16,18).

For phasing analysis the relative mobilities were plotted as a function of the distance between intrinsic and NeP1 induced bend centers. The best fit curve was assembled by PlotIt and used for calculating bending direction and bend angle (14,15,17). The bend angle α was estimated by the equation

$$\alpha = 2[\text{inv.tan.}(0.5A_{PH}/\tan 27)]$$

introduced by Kreppola and Kurran (16,18) where A_{PH} is the phasing amplitude.

RESULTS

In vitro reconstitution of the silencer protein complex

In order to analyze the *in vitro* DNA conformation within the silencer protein complex, an *in vivo*-like composition of silencer factors bound to the DNA had to be established. Therefore, we studied the DNA binding of all three proteins NeP1, TR and RXR, involved in synergistic transcriptional repression of the chicken lysozyme silencer (2–4,19–21).

First we tested the DNA binding of individual fractions one by one with the F1/F2-containing probe to analyze the resolution and specificity of all resulting bands (Fig. 1). The TR is detectable as a monomer and homodimer complex bound to the F2 element (lane 2) as has been shown previously (21). To demonstrate specificity of the TR complexes, a high affinity TR-binding oligonucleotide (4,22) containing a repeated binding site spaced by 4 nt (DR4) was used for competition. Both complexes are sensitive to competition with DR4 (Fig. 1, lane 3), in contrast with the competition with the non-TR binding F1 sequence (lane 4). In addition, TR homodimers are specifically identified by their reduced DNA binding affinity in the presence of the T3 ligand (23), as can be seen in lane 5. The combination of TR and RXR leads to one additional band that can be competed with DR4 (lanes 6 and 7). The slower migration of the TR–RXR complex is due to the higher molecular weight of RXR (22,23). Again, addition of T3 only reduces the homodimeric TR complex (lane 9).

Purifed NeP1 generates a major retarded complex in addition to a complex of higher mobility (3,19) (Fig. 1, lane 10). Both can be competed with the specific binding site (F1) (lane 11). In the presence of TR, NeP1 forms two additional slower migrating complexes, which can be identified as NeP1–TR monomer and NeP1–TR–TR homodimer by their sensitivity to DR4 competition (lane 14) or F1 competition (lane 13). Again, the TR homodimer within the NeP1–TR–TR complex is abolished by T3 (lane 19). Further addition of RXR yields the slowest migrating complex (NeP1–TR–RXR in lane 15), which is sensitive to F1 or DR 4 competition (lanes 16 and 17), but not to competition with a glucocorticoid receptor binding site (GRE, lane 18) nor to T3 incubation (lane 19). Since RXR is *in vitro* translated and TR

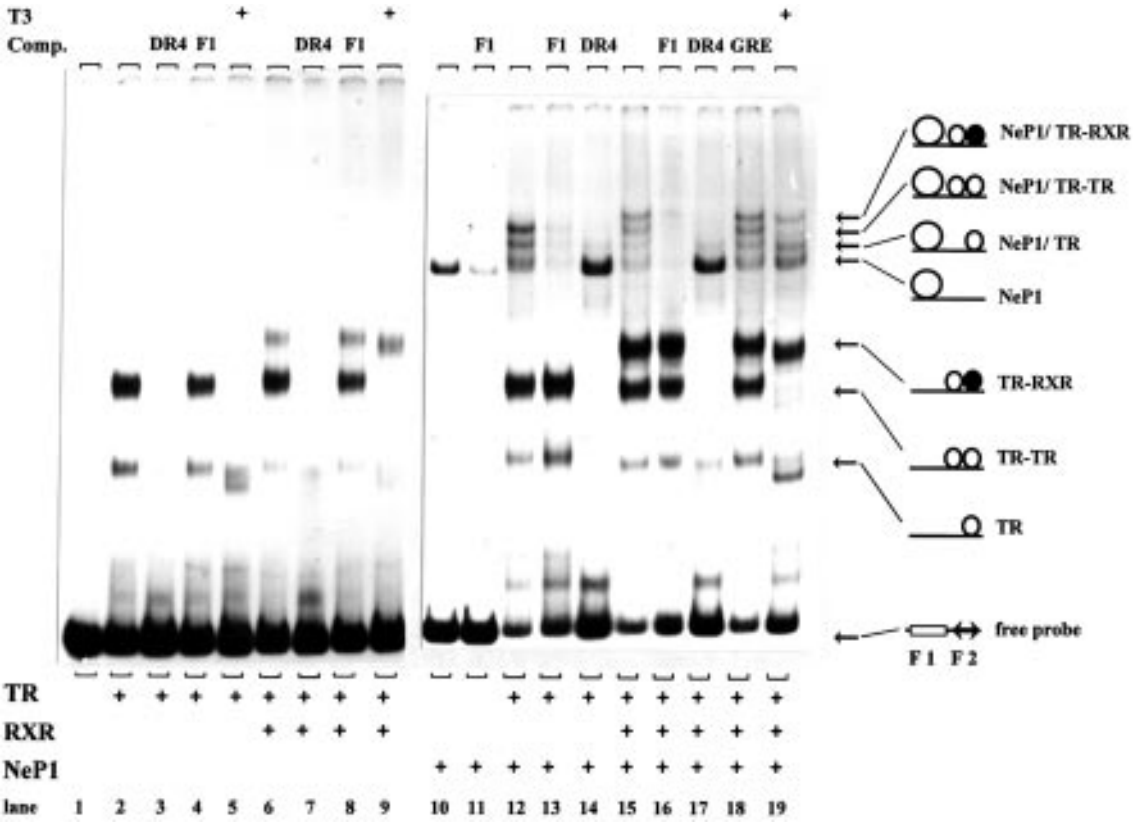

Figure 1. EMSA experiments resolve all possible complexes on the F1/F2 silencer. The ^{32}P-labelled *Bss*HII fragment was incubated with different combinations of TR-, RXR- or NeP1-containing extracts (as indicated below the lanes). The source for TR was hTRα1 expressed in *E.coli*, for RXR *in vitro* translated hRXRα, and for NeP1 highly enriched HeLa NeP1 was added. DNA competitions were carried out as indicated above the lanes with a 200-fold excess of unlabelled DR4 or F1 oligonucleotide. Thyroid hormone effects were tested by adding 10^{-5} M T3 in lanes 5, 9 and 19. The composition of each of the generated complexes is indicated on the right. The negative control (lane 1) shows the probe after incubation with a mixture of unlabelled, unprimed reticulocyte lysate and of a protein extract from non-expressing *E.coli* cells.

expressed in *E.coli*, a mixture of unlabelled, unprimed reticulocyte lysate and of a protein extract from non-expressing *E.coli* cells has been tested and shown to be free of any shifting activity (lane 1). Therefore, this system allows us to demonstrate the influence on the DNA structure, by each factor alone or in combination.

Different silencer protein complexes induce different DNA flexure angles

To identify changes on DNA conformation caused by any of the protein complexes, we analyzed their mobility by circular permutation analysis (14,15,17). The DNA constructs were cut with different restriction enzymes as indicated (Fig. 2A). This results in DNA fragments of identical length with the F1/F2 sequence placed in various positions along the length of the fragment. A bend in a DNA fragment will be detectable, because its migration in a native polyacrylamide gel is determined by the three-dimensional distance of both ends. The permutated DNA fragments were incubated with NeP1, TR and RXR (Fig. 2B). This results in a pattern of seven complexes as identified above. All of the four NeP1-containing complexes show a migration specificity dependent on the permutated probe used.

All complexes lacking NeP1 do not show any bending, except for the *Sal*I fragment which exhibits a higher mobility for the complexes lacking NeP1. This is probably due to the proteins binding to the very tip of the DNA of this particular probe (see Fig. 2A) resulting in a 'head-on' migration through the gel with the protein complex pulled behind. This non-bending of TR, TR–TR or TR–RXR on the F2 element is obvious from the calculated plots of this experiment (see below, Fig. 2C). Thus, TR monomer, homodimer or RXR heterodimer do not bend DNA on the F1/F2 silencer.

The relative mobilities of each complex were plotted as the best fit to a cosine function (Fig. 2C). Using circular permutation analysis it is not possible to discriminate between a directed bend and a higher flexibility of the DNA caused by the bound protein. Therefore, we will use the term DNA flexure angle for the result of this assay. The DNA flexure angle was calculated to be 100° in the case of NeP1 bound to DNA. When TR was bound either as a monomer, a homodimer or a heterodimer with RXR in conjunction with NeP1, the DNA flexure angle was diminished to 92–90°. The addition of T3 did not change the DNA flexure angle (data not shown). The bend centers can be calculated for each of the bending complexes as the points of maximal mobility determined from the minima of the curves shown in Figure 2C. The bending center is located upstream (distal from F2) of the F1 center, when NeP1 is the only protein bound. The analysis of six independent experiments determined a position of –16.1 bp (±0.02) upstream of the F1 center. In the presence of the TR or RXR together with NeP1, the location of the bend center is shifted

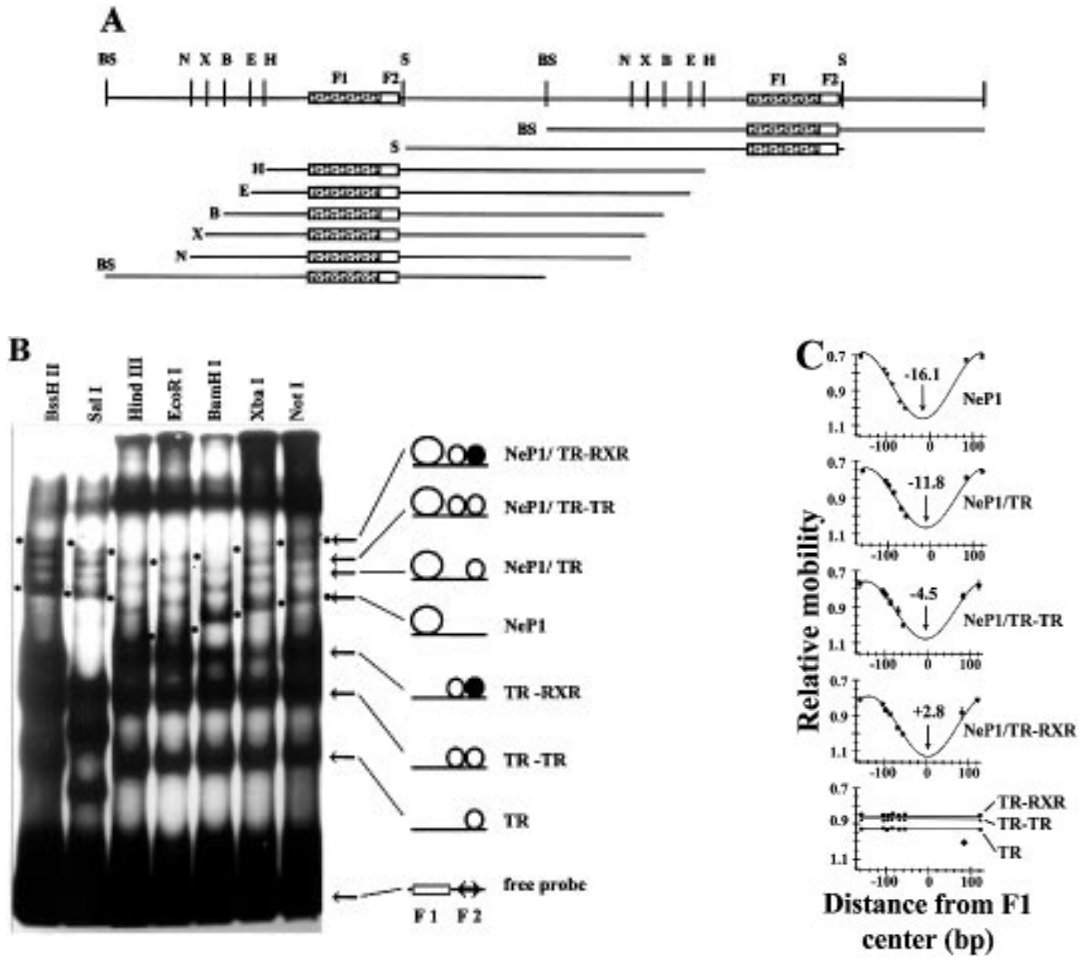

Figure 2. Circular permutation analysis of NeP1, hTRα1 and hRXRα binding to the F1/F2 silencer. (**A**) Permutated probes used containing the F1/F2 sequence in variable positions relative to the ends of the fragments. The NeP1 binding site is shaded (F1). The restriction enzymes used were*Bss*HII (BS), *Sal*I (S), *Hin*dIII (H), *Eco*RI (E), *Bam*H1 (B), *Xba*I (X) and *Not*I (N). (**B**) EMSA of NeP1, hTRα1 and hRXRα binding to the ^{32}P-labelled permutated probes generated by the indicated restriction enzymes. The assignment of the different complexes are shown on the right and are identical to Figure 1. (**C**) Best fit of cosine function for each of the complexes. Shown are the results of six independent experiments with every point representing the mean value and the indicated standard error bar. It was not possible to plot the error bar for some results because of extreme minimal variations. For each curve, the position of the bend center was determined and expressed in base pairs relative to the middle of the F1 sequence. Negative values indicate a position upstream of the middle of the F1 sequence (distal from the F2 element). The non-bending TR–RXR, TR–TR and TR shifts are summarized in a single graph (bottom of figure). In this graph a single value (diamond) is identical for all three protein complexes (see text for discussion).

towards the F2 element. The TR monomer complex with NeP1 shows a bend center at –11.8 (±0.02) bp and the NeP1/TR–TR at –4.5 (±0.03) bp upstream of the F1 center. When NeP1 bends DNA in the presence of TR–RXR heterodimer the bend center is located at +2.8 (±0.02) bp downstream of the F1 center. Exactly the same position has been determined previously as a site of DNase I hypersensitivity by *in vitro* footprinting (2).

NeP1 induces a directed bend on the DNA

To investigate whether the NeP1 induced DNA flexure angle is at least in part caused by a directed bend, a phasing analysis was carried out. A tract of six adenine residues is known to bend DNA with an angle of 18–21° (14). Accordingly, three phased A-tracts bend DNA with an angle of 54°. The resulting bend is always directed to the minor groove. DNA constructs were generated by inserting this triple A-tract region upstream of the F1/F2 element. This defined A-tract region was phased around the helical axis by inserting 2, 4, 6, 8, 10 and 12 bp as a spacer between the intrinsic A-tract bend and the F1/F2 sequences. If analyzed on a native polyacrylamide gel, the resulting complexes will migrate faster when both bends are oriented opposite to each other or will be retarded when the induced and intrinsic bends are in phase with each other.

EMSA analysis with these six different probes and combinations of the three different silencer proteins were carried out. The free probes show different mobilities due to different three-dimensional end-to-end distances. The pattern of retarded complexes (Fig. 3A) was similar to that with the F1/F2 probe. The mobilities of the DNA–protein complexes were plotted as a function of the distance between both the intrinsic and NeP1-induced bend centers (Fig. 3B). When NeP1 alone is bound to the set of six different constructs, the distance between both bend centers covers a range from 68 to 78 bp, with a maximal mobility at 76 bp (≅ 7.25 helical turns

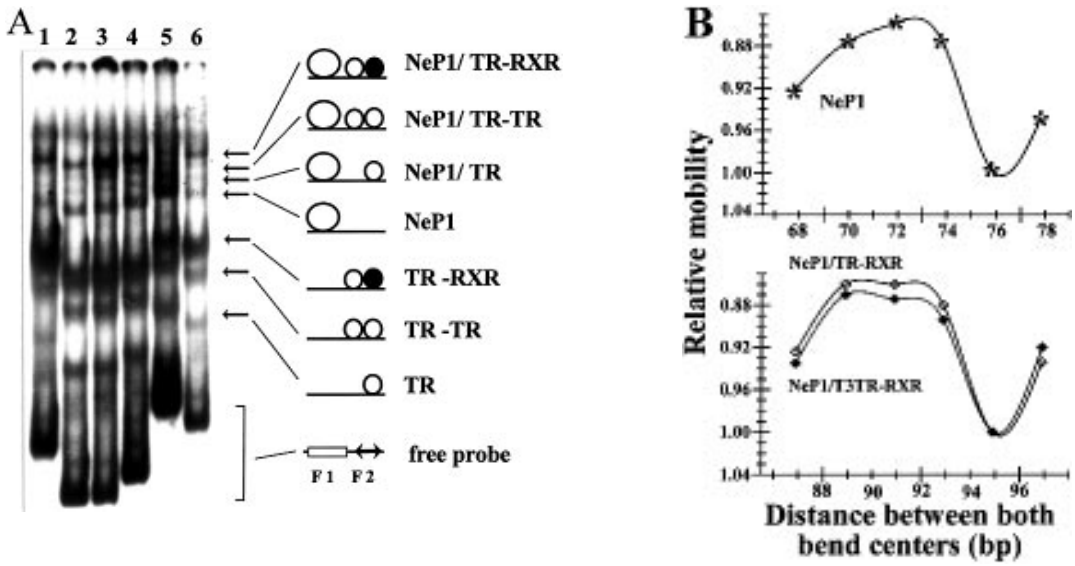

Figure 3. Phasing analysis of NeP1, hTRα1 and hRXRα binding to the F1/F2 silencer. (**A**) EMSA experiment with all three proteins (compare Fig. 1) binding to a ^{32}P-labelled probe containing the silencer and a pre-bent A-tract region spaced by 9, 11, 13, 15, 17 or 19 bp (lanes 1–6 respectively). The resolution of the different complexes is the same as for the permutated probe (Fig. 1) with the assignment of complexes shown on the right. (**B**) Graph of the direction and magnitude of the NeP1 or the NeP1–TR–RXR complex. The relative mobilities of the different complexes are plotted against the distance. This distance is taken from the center of the intrinsic bend to the center of the induced bend. Relative mobilities of the NeP1–TR–RXR complex in the absence of hormone (open symbols) or in the presence of T3 (filled symbols).

distance). Therefore, the center of the NeP1-induced bend is oriented towards a direction between major and minor groove.

In the case of the NeP1–TR–RXR complex the distance between induced and intrinsic bend centers varies from 87 to 97 bp with a maximal mobility at 95 bp (≅ 9 helical turns). This locates the induced bend center opposite to the intrinsic bend center with a direction towards the major groove. Thus, the presence of the TR–RXR heterodimer modulated a change in orientation of the induced bend. The phasing analysis (Fig. 3A) for the NeP1–TR and NeP1–TR–TR complexes (plots not shown) reveals maximal mobility at a bend-to-bend distance of 80 bp (≅ 7.6 helical turns) and 87 bp (≅ 8.3 helical turns) respectively. Using the phasing analysis to calculate bend angles, the values differ remarkably from the DNA flexure angle calculation as reported by others (18,22). For NeP1 the directed bend angle can be calculated to be 18°, for the NeP1–TR–RXR complex it is 15°, and for TR, TR–TR or TR–RXR no bending was detected (see Fig. 2C).

We wondered whether the presence of ligand might change the direction of the bend angle. The phasing analysis was carried out in the presence of T3 (data not shown). The result was plotted as the best fit to a curve function and compared for each complex (Fig. 3B). The mobility of all T3 containing complexes is slightly increased, and as expected, the TR homodimers are reduced in their binding affinity. However, the minimal or maximal mobilities of the fragments do not vary between the unliganded and liganded state. Therefore, at least in this *in vitro* DNA binding assay the presence of T3 does not change the direction of the bend.

In addition to the DNA binding domain other protein domains are required for bending

In order to analyse the functional properties of NeP1 in detail we isolated and microsequenced NeP1 (Burcin, Lottspeich, Arnold, Runge and Renkawitz, in preparation). The sequencing results and all of the tested binding properties demonstrated that human NeP1 is identical to chicken CTCF. Therefore, we used the chicken CTCF c-DNA clone (12) to express the chicken protein in COS-cells. In order to compare the bending properties of CTCF with NeP1, we selected three of the permutated DNA fragments (Fig. 2A), showing the largest difference in complex retardation for NeP1 (see Fig. 2B). These probes were incubated with extracts from untransfected COS-cells, from COS-cells expressing CTCF and for comparison with purified NeP1 (Fig. 4A). All of the three protein sources (the endogenous COS-protein, CTCF and NeP1) generate the same probe specific retardation. Since the DNA binding domain of CTCF is quite complex (11 zinc fingers), we wondered whether the DNA binding domain by itself would be sufficient for DNA bending. Therefore, we expressed just the zinc finger domain of CTCF in COS cells and used this extract with all of the circular permutation probes (Fig. 4B). None of the probes used show any indication of DNA bending by the zinc finger domain (CTCF-DBD), whereas the endogenous full-length COS-NeP1 protein mediates the expected bending. The plot of the migration mobilities (Fig. 4C) confirms this striking difference between the non-bending zinc finger domain and the 100°-bending of the full-length protein. Relative affinity measurements of the respective proteins binding to the F1 sequence (data not shown) indicate that the loss of DNA bending by the DNA binding domain is not caused by a loss in DNA affinity, rather the full length protein and the DNA binding domain have similar affinities.

DISCUSSION

The chicken lysozyme gene is regulated by several regulatory elements. One is the –2.4 kb silencer, which consists of the two modules F1 and F2. Here we analyzed whether the proteins

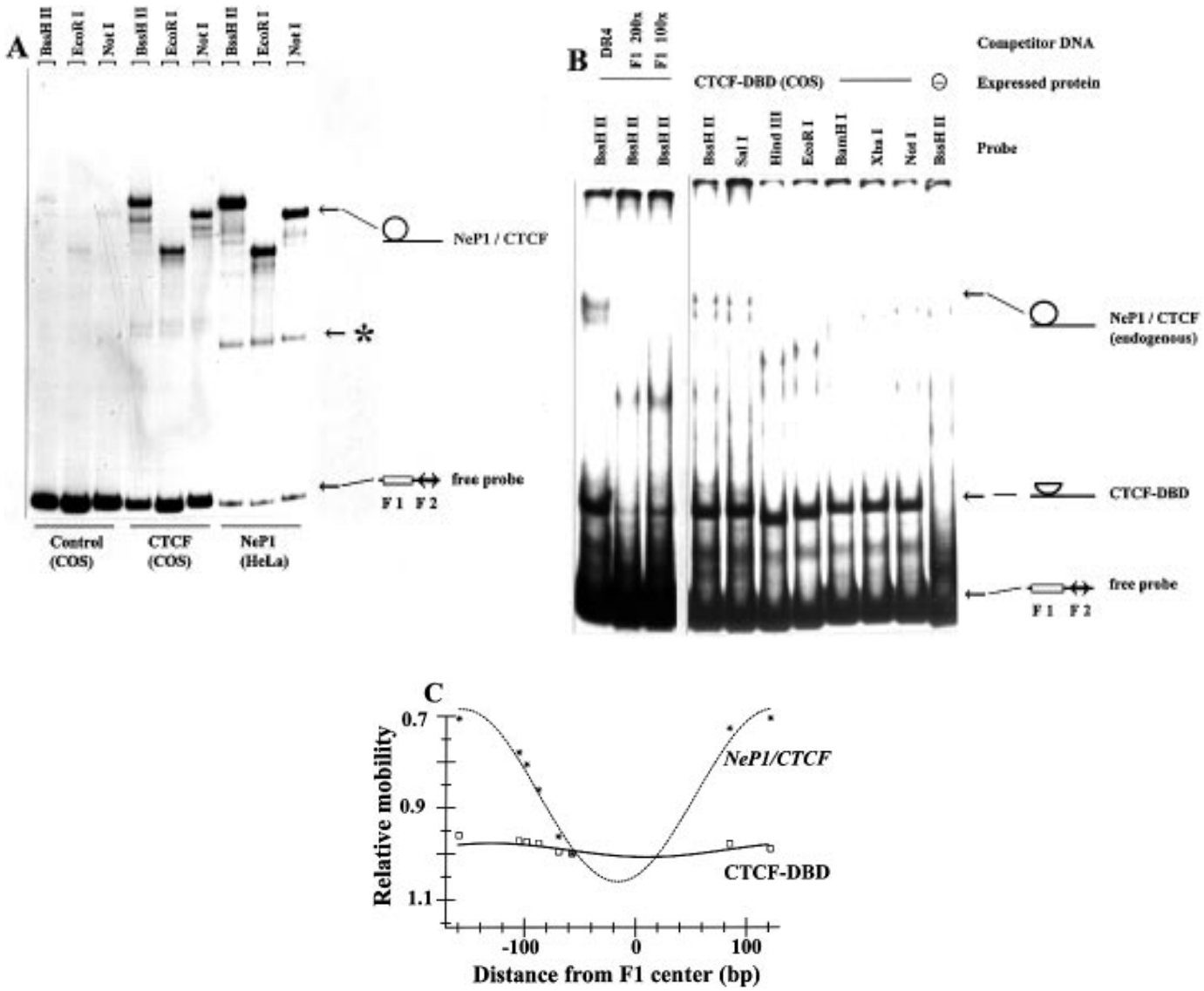

Figure 4. CTCF DNA binding domain is not sufficient for bending. (**A**) DNA bending mediated by COS cell extract, by an extract from COS cells transfected with an expression vector for CTCF, and by purified NeP1 (indicated below the lanes). All of the three protein sources generate the same complex, dependent on the specific probe used (*Bss*H, *Eco*RI or *Not*I, compare with Fig. 2A and B). Complex intensity seen with the control (COS) extract is very weak, since neither the extract was fractionated, nor an expression plasmid was used. The complex labelled with a star is a proteolytic degradation product from the isolated NeP1 protein. (**B**) COS cell extract from cells without transfected expression plasmid (see right-most lane) and from cells expressing the CTCF DNA binding domain (CTCF-DBD) was used (first four lanes on the left) and either competed with unspecific DNA (DR4) or with specific DNA (F1). The same extract from transfected cells was used with different probes (*Sal*I, *Hin*dIII, *Eco*RI, *Bam*HI, *Xba*I, *Not*1, as in Fig. 2A and B). The complex identification is shown on the right. COS cells show two specifically retarded complexes, with the upper one co-migrating with the complex generated from purified HeLa–NeP1 (compare A). (**C**) Best fit of cosine function for the CTCF-DBD complex in comparison to the NeP1–DNA complex (NeP1–CTCF, these data are taken from Figure 2C, for comparison).

binding to these elements may effect the DNA conformation. The silencer protein NeP1 generates a DNase I footprint of ~50 bp (3) and induces DNA flexibility with a flexure angle of 100°. This induced bend is not located in the center of the F1 sequence, but rather it is found ~16 bp outside of the center, distal from the F2 element. Since NeP1 binds as a monomeric protein to a sequence showing no sequence repetition, such as palindromic or direct repeats, a possible position for the bend center cannot be predicted from the sequence.

The second module (F2) has been shown to be a response element for the thyroid hormone and the retinoic acid receptor (2,4,5). This element has an everted palindromic structure in contrast with other thyroid hormone response elements with a directed repeat or a palindromic structure. The F2 element has been shown to be preferentially bound by a thyroid hormone receptor homodimer in the absence of hormone, whereas in the presence of T3 a thyroid hormone receptor–RXR heterodimer is bound (5,23,24). In contrast with DNA bending observed with TR homodimers and heterodimers with RXR on the direct repeat element spaced by 4 nt (22), the F2 element is not bent by TR homo- or heterodimers (Fig. 2). Although the presence or absence of T3 shifted the complexes from heterodimers to homodimers, in no

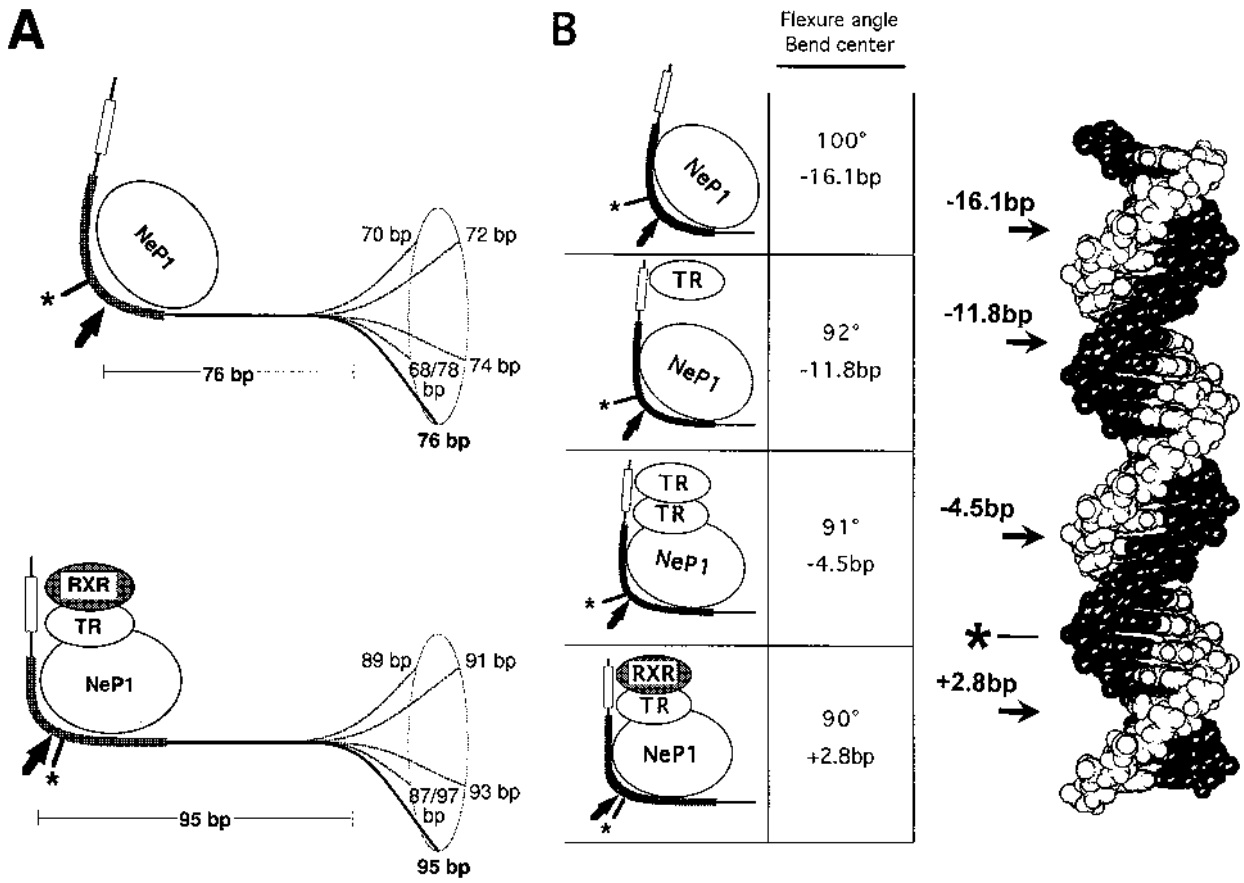

Figure 5. Summary of the DNA conformation changes in the different silencer complexes. (**A**) DNA bending by NeP1 or by the NeP1–TR–RXR complex leads to different positions of the induced bending center relative to a given distance to an intrinsic DNA bend. Since the spacer region between the two bend centers varies in the different DNA constructs by 2 bp each, these different positions of the intrinsic bend center result in different orientations of the DNA tip (indicated in the right of the figure). The protein induced bend centers are indicated by an arrow which is positioned relative to the center of the F1-sequence (*). (**B**) The positions of the bend centers and the induced flexure angles are shown. The different complex compositions are depicted on the left visualizing the bend angle and the position of the bend center (arrow) relative to the middle of the F1 sequence (*). NeP1 bound to the F1 sequence (shaded region) and TR complexes bound to the F2 element (open box) are indicated. Values for the DNA flexure angle and the bend center positions are summarized in the central column. Bend center positions relative to the DNA molecule are shown on the right.

case was a bending effect on the DNA observed. Similarly, the estrogen receptor has been shown to bend the DNA, and in the presence or absence of ligand did not change the bending properties (25).

Binding of different TR complexes together with NeP1 did not change the magnitude of the DNA flexure angle (Fig. 5), but the position of the bend center shifted within a range of ~20 bp. This shift was from position –16 bp relative to the center of the F1 sequence in case of NeP1 binding to –12 bp (NeP1–TR monomer), to –4.5 bp (NeP1–TR homodimer) and finally to + 3 bp in case of the NeP1–TR–RXR complex (Fig. 5B). The position of the bend center in case of the NeP1–TR–RXR complex at +3 bp is identical to the position of the DNase I hypersensitive site in NeP1 footprinting experiments (2,3). Whether just the bending causes the hypersensitivity or whether the specific NeP1 binding induces the hypersensitivity and thereby moves the bend center to this position is not known. Simultaneously, the bending orientation is moved from a direction between major and minor groove to a bending towards the major groove in case of the NeP1–TR–RXR complex (Fig. 5B). Although the different TR complexes have no bending activities on their own, apparently they do effect overall DNA conformation within the quaternary NeP1–TR complexes. This is reminiscent of the situation described for the quaternary nucleoprotein complex at the c-fos promoter (6). Although the binding of an ets domain from the transcription factor Elk 1 does not induce DNA bending, recruitment of Elk 1 to form a ternary complex effects the SRF-induced directional bend. Thus, in case of ELK–SRF and of NeP1–TR complexes DNA bending of the ternary complex is different from a situation where all of the binding proteins contribute independently of each other to the overall bending. The latter activity has been reported in several other cases (26–31).

The chicken homologue (CTCF; 12) of the human NeP1 showed the identical bending properties as NeP1. Analysis of the DNA binding domain revealed that the DNA bending activity is mediated by other domains in addition to the DNA binding domain. A similar result has been seen with the orphan nuclear receptor RORα, which induces a significant bend in the DNA, whereas the DNA binding domain of this protein results in a decreased angle of the bent DNA (32). This finding may be explained by an influence of neighbouring domains on the orientation of the zinc fingers.

Several different functions for bent DNA have been proposed and in some cases these functions were experimentally confirmed. One function might be that the conformational distortion of the DNA would by itself have a regulatory role such as looping distant regulatory elements into a proximal conformation. In such a case, a DNA sequence containing an intrinsic bend should have a similar function as the bending protein (33). This does not seem to be the case for the lysozyme silencer sequence, since the transcription inducing complex (NeP1–TR–RXR + T3) shows a similar overall bending as the repressor complex seen in the absence of T3 (NeP1–TR–TR). For another repressor complex, the a1-α2 homeodomain proteins from yeast also induce bending, but a DNA bend by itself does not seem to be sufficient for repression (34).

Another function might be that within a quaternary complex, the bending factor may induce cooperative binding of a second factor, which may require a pre-bend DNA. This seems to be the case for TBP and TFIIB (7). Again, at least *in vitro* cooperative binding, is not observed for the lysozyme silencer. Here we show in the electrophoretic mobility shift assays independent binding of NeP1 and TR complexes.

For some enhancer complexes it has been shown, that DNA bending serves an architectural role in assembling a higher order complex of proteins which in this arrangement may interact optimally with the transcription machinery (27–31). It may be possible that such a prebuilt multicomponent complex might allow optimal interaction with the transcription machinery in the case of the lysozyme silencer in the absence of ligand as well as optimal induction in the presence of T3. Synergy in repression and synergy in induction have been demonstrated for the F1 and F2 modules (2). The silencing complex (NeP1–TR–TR homodimer; predominant form in the absence of ligand) and the enhancing complex (NeP1–TR–RXR; predominant form in the presence of ligand) show almost identical DNA flexure angles and only slightly shifted positions of their bend centers. Interestingly, the enhancing complex is the only one bending the DNA towards the major groove, whereas all other NeP1 complexes bend the DNA towards a direction in between major and minor grooves (Fig. 5B). In addition to providing a three-dimensional surface of proteins interacting with the transcription machinery, DNA bending may control nucleosomal phasing and/or nucleosomal binding in the presence of the silencer proteins. Future experiments will determine which of the above mechanisms are relevant for the lysozyme silencer.

ACKNOWLEDGEMENTS

We are grateful to L. Schäfer-Pfeiffer for excellent technical assistance, to M. Hollenhorst for help with the mathematical calculations, to R. Niedenthal for providing the pre-bent vectors, and to L. J. DeGroot for pET-hTRα1 and E. M. Klenova for pS65-CTCF. Also we would like to thank A. Baniahmad and M. Short for critically reading the manuscript. This work contains parts of the Ph.D. thesis of R. Arnold. The work was supported by grants from the Sonderforschungsbereich 272 and from the Fond der Chemischen Industrie.

REFERENCES

1 Sippel,A.E., Theisen,M., Borgmeyer,U., Strech-Jurk,U., Rupp,R.A.W., Püschel, A.W., Müller,A., Hecht,A., Stief,A. and Grusemeyer,T. (1988) In Kahl,G., (ed.), *Architecture of Eukaryotic Genes.* VCH Verlagsgesellschaft, Weinheim, pp 355–369.
2 Baniahmad,A., Steiner,C.H., Köhne,A.C. and Renkawitz,R. (1990) *Cell*, **61**, 505–514.
3 Köhne,A.C., Baniahmad,A. and Renkawitz,R. (1993) *J. Mol. Biol.*, **232**, 747–755.
4 Ikeda,M., Rhee,M. and Chin,W.W. (1994) *Endocrinology*, **135**, 1628–1638.
5 Williams,G.R., Zavacki,A.M., Harney,J.W. and Brent,G.A. (1994) *Endocrinology*, **134**, 71888–71896.
6 Sharrocks,A.D. and Shore,P. (1995) *Nucleic Acids Res.*, **23**, 2442–2449.
7 Lee,S. and Hahn,S. (1995) *Nature*, **376**, 609–612.
8 Dignam,J.D., Lebovitz,R.M. and Roeder,R.G. (1983) *Nucleic Acids Res.*, **11**, 1475–1489.
9 Shapiro,D.J., Sharp,P.A., Wahli,W.W. and Keller, M.J. (1988) *DNA*, **7**, 47–55.
10 Studier,F.W., Rosenberg,A.H., Dunn,J.J. and Dubendorff,J.W. (1990) *Methods Enzymol.*, **185**, 60–89.
11 Mangelsdorf,D.J., Umesono,K., Kliewer,S.A., Borgmeyer,U., Ong,E.S. and Evans,R.M. (1991) *Cell*, **66**, 555–561.
12 Klenova,E.M., Nicolas,R.H., Paterson,H.F., Carne,A.F., Hath,C.M., Goodwin,G.H., Neiman,P.E. and Lobanenkov,V.V. (1993) *Mol. Cell. Biol.*, **13**, 7612–7624.
13 Niedenthal,R.K., Sen-Gupta,M., Wilmen,A. and Hegemann,J.H. (1993) *Nucleic Acids Res.*, **21**, 4726–4733.
14 Thompson,J.F. and Landy,A. (1988) *Nucleic Acids Res.*, **16**, 9687–9705.
15 Kreppola,T.K. and Curran,T. (1991) *Cell*, **66**, 317–326.
16 Kreppola,T.K. and Curran,T. (1991) *Science*, **254**, 1210–1214.
17 Kreppola,T.K. and Curran,T. (1993) *Mol. Cell. Biol.*, **13**, 5479–5489.
18 Lu,X.P., Eberhardt,N.L. and Pfahl,M. (1995) *Mol. Cell. Biol.*, **13**, 6509–6519.
19 Burcin,M., Köhne,A.C., Runge,D., Steiner,C. and Renkawitz,R. (1994) *Seminars in Cancer Biology*, **5**, 337–346.
20 Wahlström,G.M., Sjoberg,M., Andersson,M., Nordström,K. and Vennström,B. (1992) *Mol. Endocrinol.*, **6**, 1013–1022.
21 Andersson,M.L., Nordström,K., Demczuk,S., Habers,M. and Vennström,B. (1992) *Nucleic Acids Res.*, **20**, 4803–4810.
22 Shulemovich,K., Dimaculangan,D.D., Katz,D. and Lazar,A. (1995) *Nucleic Acids Res.*, **23**, 811–818.
23 Ribeiro,R.C.J., Kushner,P.J., Apriletti,J.W., West,B.L. and Baxter,J.D. (1992) *Mol. Endocrinol.*, **6**, 1142–11528.
24 Yen,P.M., Brubaker,J.H., Apriletti,J.W., Baxter,J.D. and Chin,W.W. (1994) *Endocrinology*, **134**, 1075–1081.
25 Nardulli,A.M., Grobner,C. and Cotter,D. (1995) *Mol. Endocrinol.*, **9**, 1064–1076.
26 Kudduz,R., Gu,B. and DeLuca,N.A. (1995) *J. Virol.*, **69**, 5568–5575.
27 Sheridan,P.L., Sheline,C.T., Cannon,K., Voz,M.L., Pazin,M.J., Kadonaga,J.T. and Jones,K.A. (1995) *Genes Dev.*, **9**, 2090–2104.
28 Love,J.J., Li,X., Case,D.A., Giese,K., Grosschedl,R. and Wright, P.E. (1995) *Nature*, **376**, 791–795.
29 Giese,K., Kingsley,C., Kirshner,J.R. and Grosschedl,R. (1995) *Genes Dev.*, **9**, 995–1008.
30 Falvo,J.V., Thanos,D. and Maniatis, T. (1995) *Cell*, **83**, 1101–1111.
31 Thanos,D. and Maniatis,T. (1995) *Cell*, **83**, 1091–1100.
32 McBroom,L.D.B., Flock,G. and Giguère,V. (1995) *Mol. Cell. Biol.*, **15**, 796–808.
33 Meacock,S., Pescini-Gobert,R., DeLamarter,J.F. and Hooft-van-Huijsduijnen, R. (1995) *J. Biol. Chem.*, **269**, 31756–31762.
34 Smith,D.L., Desai,A.B. and Johnson,A.D. (1995) *Nucleic Acids Res.*, **23**, 1239–1243.